



Evaluation of microtiter plate as a high-throughput screening platform for beer fermentation

Xiangdong Zhao¹ · Roland Kerpes¹ · Thomas Becker¹

Received: 23 November 2021 / Revised: 17 March 2022 / Accepted: 19 March 2022 / Published online: 22 April 2022
© The Author(s) 2022

Abstract

Downscaling the anaerobic fermentation in a microtiter plate (MTP) facilitates high throughput screening (HTS) applications. This study investigates the impacts of MTP configurations (scale, shaking, and cover) on the *S. pastorianus* beer fermentation compared to that in the shaking flask (SF) and European Brewing Convention (EBC) tube regarding fermentation performances and flavor attributes. The lager strains in MTPs accelerated cells reproduction and vitalization, sugar consumption, and glycerol accumulation. The microscale beer fermentation was closer to the SF but differed greatly from EBC tube fermentation depending on the MTP configurations. The downscaling from 2 mL to 0.2 mL in MTP increased the cell growth rate and vitality but did not change the maximum cell density. The shaking MTP did not promote early growth but sustained significantly higher cell numbers at the later fermentation stage. More than 1.5-folds acetaldehyde and higher alcohols, yet less than half esters, were obtained from the MTP and SF fermentations relative to that in the EBC tube. The air-tight MTP cover, as compared to the gas-permeable cover, not only balanced the above volatile flavors but also maintained integrity to the endogenous carbon dioxide pressure during beer fermentation. Additionally, fermentative activities were reduced by excluding air in either the material or the headspace of MTP. Hence, MTP configurations influenced *S. pastorianus* beer fermentation. These influences were partly attributed to their impacts on air accessibility. Conscious of the impacts, this study helps interpret the minimized fermentation and sheds light on the development of MTP based HTS platform for anaerobic cultivations.

Keywords Yeast · Fermentation · Microtiter plate (MTP) · High-throughput screening (HTS) · Flavor · Beer

Introduction

High-throughput screening (HTS) has been applied in a broad range of microbial cultivation [1–4]. Microtiter plate (MTP) is often adopted as the minimized culture vessel for the HTS applications for its cost-effective and automation compatibility [5]. The MTP cultivations were successfully scaled up to bench bioreactors regarding the biomass development, the nutrient consumption, and the production of organic acids [2, 6], proteins [4, 7], lipids [1, 8], and other

metabolites by various bacteria and fungi strains [3, 9, 10]. Nevertheless, most validations were made for aerobic cultivations, at which MTP configurations concerning well geometry, material, and surface [11, 12], filling volume and shaking parameter [13, 14], as well as cover designs [15–17] have been optimized to ensure sufficient oxygen supply to stimulate cell growth. In contrast, these specifications were rarely customized for anaerobic fermentation [5, 18]. The MTP anaerobic fermentation was realized via two strategies: one is the ‘Place in Anaerobicity’-enclosed containers filled with nitrogen or carbon dioxide were used as shelters for the MTP cultivations [18, 19]; another is the airtight sealing by mineral oil or adhesive seals [10, 18]. Deoxidizer was applied in the medium when strict anaerobiosis was required [18].

Though MTP is feasible for hosting various microbial cultures, the following configurations could challenge beer fermentation. The first and foremost challenge could be the excessive air supply in a miniaturized MTP well. The scale

✉ Xiangdong Zhao
xzhaow@wzw.tum.de

Roland Kerpes
roland.kerpes@tum.de

¹ Present Address: Institute of Brewing and Beverage Technology, Research Group Beverage and Cereal Biotechnology, Technical University of Munich, Weihenstephaner Steig 20, 85354 Freising, Germany

miniaturization increases the ratio of the headspace air to the culture volume [5]. The well surface of the cell culture plate often has oxygen atoms to stimulate cell growth [12]. The material and cover of MTP are relatively gas permeable compared to the stainless steel or glass bioreactors [20, 21]. These specifications provide more oxygen access to the cell in an MTP well than in conventional beer fermenters. Hence, a higher static oxygen transfer rate (OTR) is expected at smaller MTPs [5]. Though brewer's yeast strains are predominantly Crabtree positive, which can ferment wort under excessive air supply [22, 23], the surplus oxygen did change the course of fermentation and flavor [24–26]. Thus, the potential of using MTP for beer fermentation remains open.

The second yet contradicting challenge lies in the dilemma of shaking. The MTP minimization shortens the bubbling path [27], reduces the static shear [28, 29], and empowers the surface tension to counteract the liquid flow and movement by the diminished diameter [5, 13], all of which facilitated cell sedimentation. However, mixing is critical to avoid stagnant fermentation, especially for brewer's yeast strains with high flocculation potentials [30, 31]. Shaking MTP promotes mixing, but could also increase OTR [13, 14]. Considering the sufficient air supply in the static MTP, the effect of shaking is to be investigated for anaerobic fermentation.

The third but often neglected challenge is applying appropriate covers for anaerobic fermentation. The MTP cover is universally expected to minimize edge effects [32], prevent cross-contamination, and reduce evaporation [5]. Both gas-permeable and airtight covers, in relative terms, have been applied in beverage fermentation [10, 33]. However, none was dedicated to anaerobic fermentation concerning flavor formation. The former was designed to improve air exchange, yet the latter was designed to enhance optical transparency [16–18]. During alcoholic fermentation, CO₂ is produced and can be withheld in a sealed MTP. The enclosed system would change not only the metabolic flow and yeast physiology [34], but also pressurize the cover. Therefore, insights into the MTP cover are desired to host alcoholic fermentations.

To facilitate the HTS in beverage fermentations, this study (i) investigates the scalability of MTPs to shaking flask (SF) and European Brewery Convention (EBC) tube concerning the fermentation development, cell physiology, and flavor profile; (ii) inspect the impacts of the MTP scale (0.2, 2 mL), shaking (0, 300 rpm) and adhesive cover (gas permeable, airtight) to the non-strict anaerobic beer fermentation; (iii) evaluate the impacts of air, either in the MTP material or in the MTP headspace, on beer fermentation.

Materials and methods

Yeast, medium, and fermentation conditions

Two lager brewing strains, *S. pastorianus* TUM34/70 and TUM128 (Institute of Brewing and Beverage Technology, Technical University of Munich, Germany), were adopted to ferment the all-malt wort. Wort was prepared by dissolving the Bavaria Pilsner malt extract (Weyermann, Germany) and Hallertau Herkules CO₂-hop extract (Hopsteiner, Germany) in sterile water and manually aerated at room temperature before use. The prepared wort was in the following specifications after determination: international bittering units (IBUs), 20; apparent extract, 12.3°P; pH, 5.2; glucose, 10 g/L; fructose, 4 g/L; sucrose, 3 g/L; maltose, 78.5 g/L; maltotriose, 14.5 g/L; free amino nitrogen (FAN), 213.2 mg/L; dissolved oxygen, 8.4 mg/L.

The yeast cells were propagated progressively in the prepared wort at 26 °C at 100 rpm shaking. The cells were cropped, counted, and stored in Ringer's solution (Merck, Germany) at 4 °C less than 24 h before use. 15 million viable cells/mL were pitched in the prepared wort at room temperature. After gentle homogenization, the pitched wort was distributed in, namely, 200 µL scale in the 96-well MTP (Cat. 3596, Corning, USA), 2 mL in 24 MTP (Cat. 3526, Corning, USA), and 200 mL in 300 mL Erlenmeyer flask (Merck, Germany). The MTPs were sealed immediately with either Breathe-Easy™ (380,059, Diversified Biotech, USA) or the EASYseal™ (676,061, Greiner Bio-One, Germany) adhesive seal. They are referred to as gas permeable (polyurethane) or airtight (polyester) for their gas-permeable properties. The SF was sealed immediately with aluminum foil after distribution. All fermentation was carried out at 12 °C. The MTPs and SF were placed in a chamber with 70% humidity control at shaking or static, as listed in detail in Table 1. The 2 L EBC fermentations underwent the same propagation, but were individually pitched for all the replicates.

Samples were collected at 24 h intervals for up to 192 h in the three biological replications for the time-series analysis (Figs. 1 and 2). At each time point, probes in each column of 96 MTP and each well of 24 MTP were taken out after pipette mixing. About 2 mL was pulled out from the SF after gentle homogenization by handshaking and about 50 mL sample was withdrawn from the EBC tube via the faucet locating 40 cm from the bottom. The collected samples were firstly counted for the cell numbers, followed by centrifugation at 4 °C at 3000 rpm for 5 min to separate the cells with the broth. The sedimented cells were adopted for intracellular pH (ICP) measurement directly after the separation.

Table 1 Fermenter configuration and flavor profile of beer fermentation in MTPs, SF, and EBC tube

Attributes	A0.2	N0.2	S0.2	N2	SF	EBC
Fermenter characterization						
Vessel	96 MTP	96 MTP	96 MTP	24 MTP	Erlenmeyer flask	EBC tube
Seal	Air-tight	Gas-permeable	Gas-permeable	Gas-permeable	Aluminum foil	Aluminum foil
Shaking [rpm]	0	0	300	0	100	0
Vessel material	Polystyrene	Polystyrene	Polystyrene	Polystyrene	Borosilicate glass	Stainless steel
Diameter [cm]	0.64	0.64	0.64	1.56	8.7	5
Height [cm]	1.12	1.12	1.12	1.78	16	150
Total capacity [mL]	0.36	0.36	0.36	3.4	300	2945
Working volume [mL]	0.2	0.2	0.2	2	200	2000
Fermentation parameters						
Live cells [10^6 cells/mL]	115.8 ± 13	119.9 ± 11.5	142.8 ± 16.8	114.3 ± 8.5	147.3 ± 18.8	31 ± 1.6
Intracellular pH	5.6 ^a	5.7 ± 0.1	5.7 ^a	5.6 ^a	5.6 ^a	5.9 ^a
Medium pH	4.1 ^a	4 ^a	3.9 ^a	4.1 ^a	3.9 ± 0.1	4.3 ^a
Apparent extract [g/100 mL]	4.4 ^b	4.2 ^b	3.2 ^b	4.7 ± 0.2	4.8 ± 0.7	4.6 ± 0.4
FAN [mg/L]	102 ^b	119 ^b	124.7 ^b	115.6 ± 9	110.3 ± 5.9	132.8 ± 5.7
Flavor attributes [mg/L]						
Alcohol [vol%]	3.7 ^b	3.7 ^b	4.2 ^b	3.5 ± 0.1	3.3 ± 0.3	4 ± 0.2
Glycerol [g/L]	1.1 ± 0.1	0.8 ^a	0.7 ^a	1 ^a	0.6 ± 0.1	1 ± 0.1
Acetaldehyde	13.3 ± 2	27.9 ± 3	28.5 ± 2.3	20.6 ± 0.7	59.3 ± 8.5	9 ± 0.3
Diacetyl	1.2 ± 0.1	0.8 ± 0.1	0.7 ± 0.1	1.1 ± 0.1	0.7 ± 0.1	0.7 ± 0.2
2,3-Pentanedione	0.7 ± 0.1	0.5 ± 0.1	0.5 ± 0.1	0.7 ^a	0.7 ^a	0.5 ± 0.1
Propanol	16.1 ± 1.9	31.9 ± 4.6	20.4 ± 0.6	13.2 ± 0.4	19.1 ± 4.3	6.8 ± 0.3
Isobutanol	9.2 ± 0.5	10.6 ± 1.2	12.6 ± 0.6	9.2 ± 0.4	12.5 ± 2.7	5.4 ± 1
Isoamyl alcohol	29.4 ± 3.9	26 ± 3.8	30.3 ± 2.4	27.3 ± 1.3	4.1 ± 1.5	19.7 ± 2.8
2-Methyl butanol	8.4 ± 0.8	6.4 ± 1.1	7.4 ± 0.6	7.2 ± 0.3	28.8 ± 6.7	5.2 ± 1
Ethyl acetate	8.3 ± 1.3	4.2 ± 0.8	5.6 ± 0.9	8.1 ± 0.7	6.3 ± 0.5	14.8 ± 2.4
Isoamyl acetate	– ^c	– ^c	– ^c	– ^c	– ^c	0.8 ± 0.2

Flavors were analyzed after 144 h of undisrupted fermentation at different batches

^aData are presented as the mean ± SD, $n=3$, SD is not shown if it is 0.0

^bData are based on a single measure due to the volume limitation

^cNon-detectable

The supernatant was collected and frozen at $-20\text{ }^{\circ}\text{C}$ until further analysis.

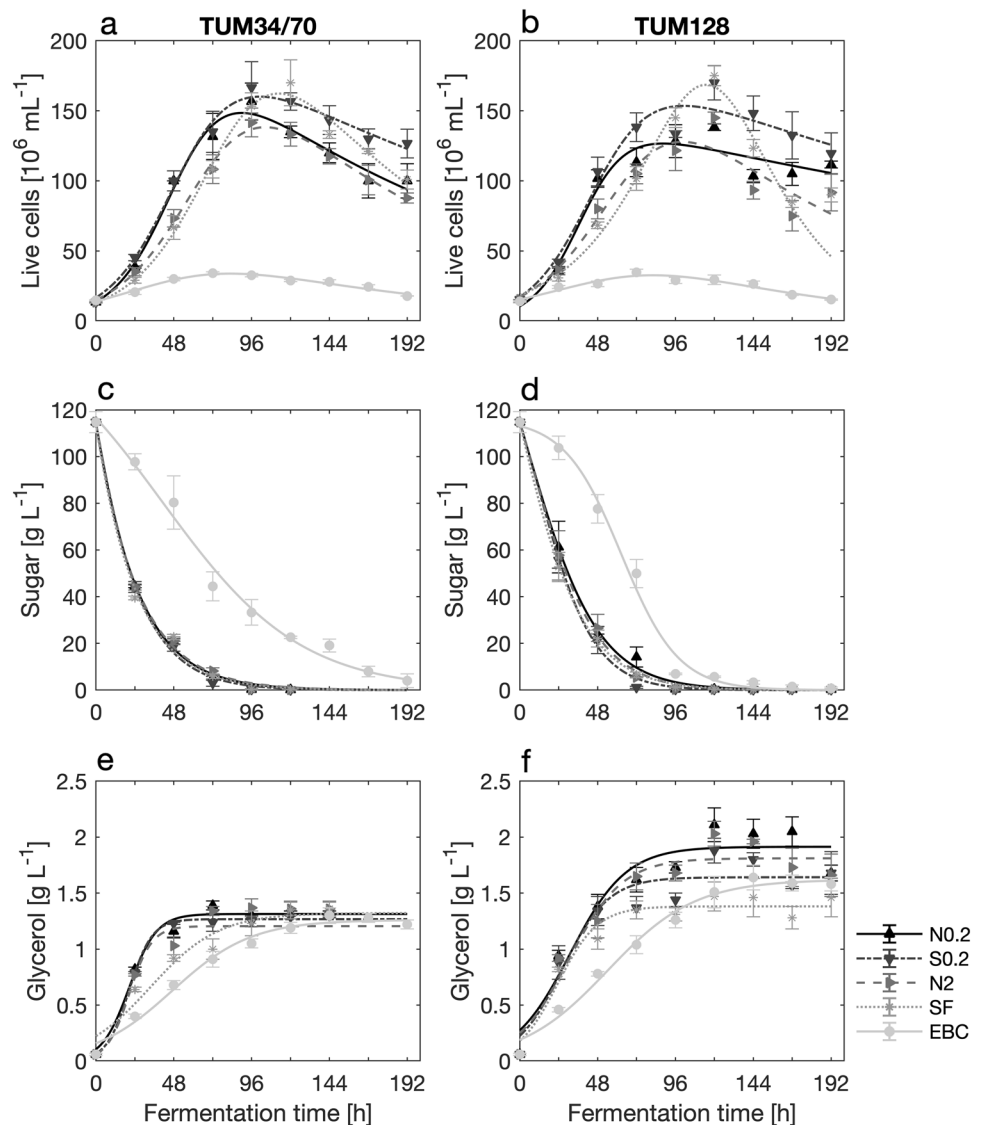
Analysis of yeast, fermentation, and flavor

The cell number and viability were determined by manual counting with methylene blue staining via a hemocytometer. Cell vitality was determined as ICP value by the flow cytometric assay using the Cell Lab Quanta™ SC Flow Cytometer (Beckman Coulter, USA) in a downscale format. Briefly, the resulting yeast pellet was washed and diluted about 20 times into 2 mL cell suspension with the loading buffer. 4 μL yeast cell dye was added to the suspension, followed by vigorous shaking and water incubation ($30\text{ }^{\circ}\text{C}$ for 15 min at dark). The cell dye's fluorescence intensity was pH dependent at 525 nm yet independent at 575 nm,

and the intensity ratio was pre-calibrated to the pH value. The ICP was averaged out of the values of 20,000 cells. The chemicals (Sigma Chemicals Co., USA), preparation, calibration, measurement, and instrument configurations have been described elsewhere in detail [35].

Wort sugar was analyzed by high-performance anion-exchange liquid chromatography with pulsed amperometric detection (HPAEC-PAD) using Dionex ICS 5000 HPLC system (Thermo Fischer Scientific, USA) equipped with ASAP autosampler and the Dionex CarboPac PA100 columns (separation column: $4 \times 250\text{ mm}$ and guard column: $4 \times 50\text{ mm}$) [36]. Depending on the fermentation time, samples were diluted 10/50/100-fold to fit in the detection ranges, which were 0.6–60 mg/L for glucose, fructose, sucrose, and 6–600 mg/L for maltose and maltotriose. The diluted sample was filtered ($\emptyset 0.45\text{ }\mu\text{m} \times 25\text{ mm}$, CHROMAFIL) into a 1 mL

Fig. 1 Logistic fit of beer fermentation in MTPs, SF, and EBC tube. *S. pastorianus* TUM34/70 (left column) and TUM128 (right column) were fermented in all-malt wort at different scales in microtiter plates (MTPs), shaking flask (SF) and EBC tall tube. The live cell numbers (a, b), sugar consumption (c, d), and glycerol accumulation (e, f) were measured offline every 24 h. Error bar indicates the mean \pm SD of three biological replications. *N0.2* 0.2 mL static fermentation in 96 standard MTP, *S0.2* 0.2 mL shaking fermentation in 96 standard MTP, *N2* 2 mL static fermentation in 24 standard MTP, *SF* 200 mL shaking fermentation in 300 mL Erlenmeyer flask, *EBC* 2 L static fermentation in the EBC tall tube



screw-cap vial for the wort sugar detection. The results were quantified by Chromeleon 6.0 software (Thermo Fisher Scientific, USA). Medium pH was measured by Orion 8220BN microelectrode (Thermo Fischer Scientific, USA) after calibration. Glycerol was assayed enzymatically (Megazyme, Ireland) in the MTP format using the Synergy™ H4 hybrid microplate reader (BioTek, Germany) and Precision™ XS pipetting robot (BioTek, Germany).

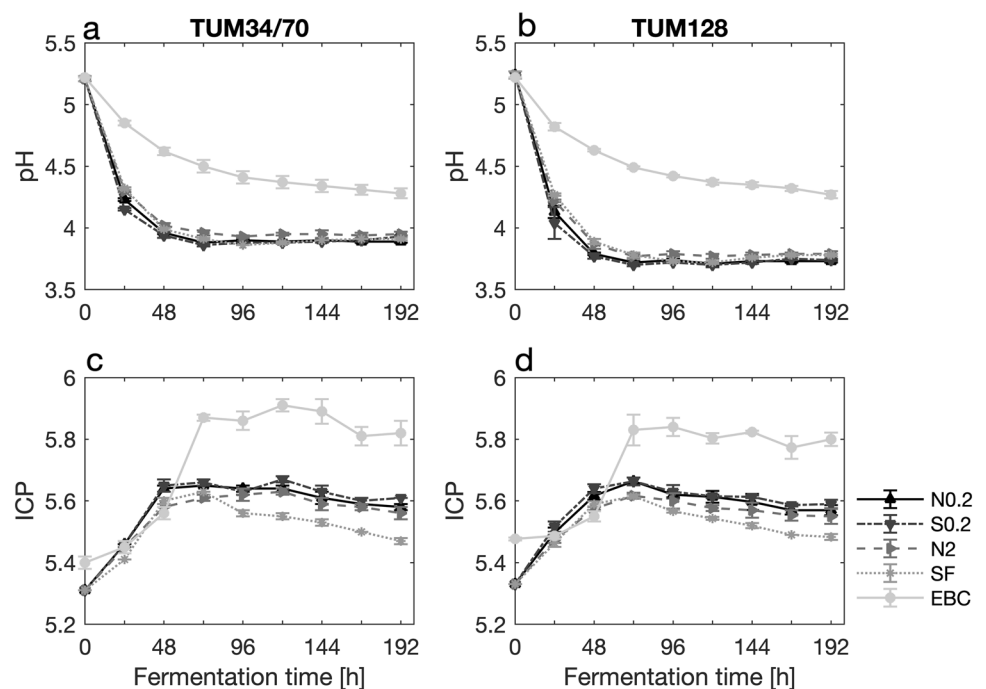
For the end-point flavor analysis, TUM34/70 fermentation samples were gathered from the whole MTPs and SF after 144 h of the uninterrupted fermentation (no in-between sampling) (Table 1). DMA 4500 density meter and AlcoLyzer plus (Anton Paar, Austria) were employed to test the extract and alcohol content. FAN was assayed photometrically by the ninhydrin method according to MEBAK 2.6.4.1 in the MTP format [37]. Higher alcohols and esters were detected with slight modification by headspace gas

chromatography with flame ionization detector (HS-GC-FID) after MEBAK 2.21.6 [38]. Vicinal diketones were determined by HP 5890 Series II Plus gas chromatography with an electron capture detector (ECD) equipped with a headspace autosampler (HP 7694; Hewlett-Packard, Germany) after MEBAK 2.21.5.1 [38]. The capillary column used for the analysis was an HP-5 column (crosslinked 5% Ph-95% Me-Si, Hewlett-Packard, Germany). The results were quantified with Agilent ChemStation Rev.A.10.01.

MTP air access control and oxygen measurement

Static 200 μL fermentations of the synthetic wort by TUM34/70 were performed to evaluate the air's impacts and the dissolved oxygen consumption in the MTP beer fermentation. The propagation, pitching, and fermentation parameters were as described without specification. The

Fig. 2 Changes of cell vitality and pH during beer fermentation in MTPs, SF, and EBC tube. *S. pastorianus* TUM34/70 (left column) and TUM128 (right column) were fermented in all-malt wort at different scales in microtiter plates (MTPs), shaking flask (SF) and EBC tall tube. Medium pH (a, b) and cell vitality in terms of intracellular pH (ICP: c, d) were measured offline every 24 h. Error bar indicates the mean \pm SD of three biological replications. *N0.2* 0.2 mL static fermentation in 96 standard MTP, *S0.2* 0.2 mL shaking fermentation in 96 standard MTP, *N2* 2 mL static fermentation in 24 standard MTP, *SF* 200 mL shaking fermentation in 300 mL Erlenmeyer flask, *EBC* 2 L static fermentation in the EBC tall tube



recipe of synthetic wort is described elsewhere [39]. The MTP (μ CLEAR[®] 655097, Greiner Bio-one, Germany) was inoculated in a sealed plastic box filled with N₂ gas for 24 h to exclude the air in the material. The control (N₂-inoculated) and the reference (air-saturated) MTPs were both covered with the airtight film for the 12 °C fermentation. Three disposable wells were assigned to each time point to measure MTP OD600 by the microplate reader and the pH. The coefficient of variation (CV%) evaluated the well-to-well variations during beer fermentation (Fig. 3a).

The oxygen consumption was tested by the OxoPlate[®] (OP96C, PreSens, Germany) covered with the airtight seal. Briefly, the sample in the sealed well was measured for the fluorescent intensity at the two wavelengths (bandwidth at 9 nm and gain at 70 nm) for the excitation to the emission ratio: 540 nm/650 nm as the oxygen-dependent indicator and the 540 nm/590 nm as the oxygen-independent reference. The intensity ratio (*I*) was calibrated to the deoxygenated (0 mg/L) and the 100% air-saturated water (8.4 mg/L) in eight replications with $R^2=0.9995$ and RMSE=0.3653. The oxygen content (mg/L) was read out from the pre-calibration by $(42.5 - I)/3.48$. Column-wise fermentations and blank controls (uninoculated synthetic wort) were also hosted next to the calibration samples in the same OxoPlate[®].

The pitching and sealing operations were performed first on the sterile bench fluxing with the filtered air and then in the glovebox fluxing with N₂ gas in the same OxoPlate[®] to fill the headspace with either air as reference or N₂ as control, respectively. The fermentations were monitored online

for MTP OD600 and oxygen consumption at room temperature (Fig. 3b). Additionally, the difference of lager brewing strains in oxygen consumption was examined in another OxoPlate[®] with a single colony incubation at room temperature in a single well. TUM34/70 and TUM128 failed for technical reasons. Instead, lager strain HTS39 and TUM164 (Institute of Brewing and Beverage Technology, Technical University of Munich, Germany) were illustrated for their oxygen consumption in correlation with cell reproduction (Fig. 3c).

Fermentation kinetics and statistical analysis

Fermentation kinetic was analyzed in MTPs, SF, and EBC tube. The dynamic of cell growth, sugar consumption, and glycerol production can be described by the following equations:

$$\frac{\Delta X}{\Delta t} = \mu' X = (\mu - kd)X, \quad (1)$$

$$\frac{\Delta N}{\Delta t} = -q_N X, \quad (2)$$

$$\frac{\Delta P}{\Delta t} = q_P X, \quad (3)$$

where $\frac{\Delta X}{\Delta t}$, $\frac{\Delta N}{\Delta t}$, and $\frac{\Delta P}{\Delta t}$ are the differences of the viable cell density X (10^6 cells/mL), fermentable sugar concentration N (g/L), and glycerol concentration P (g/L) across consecutive

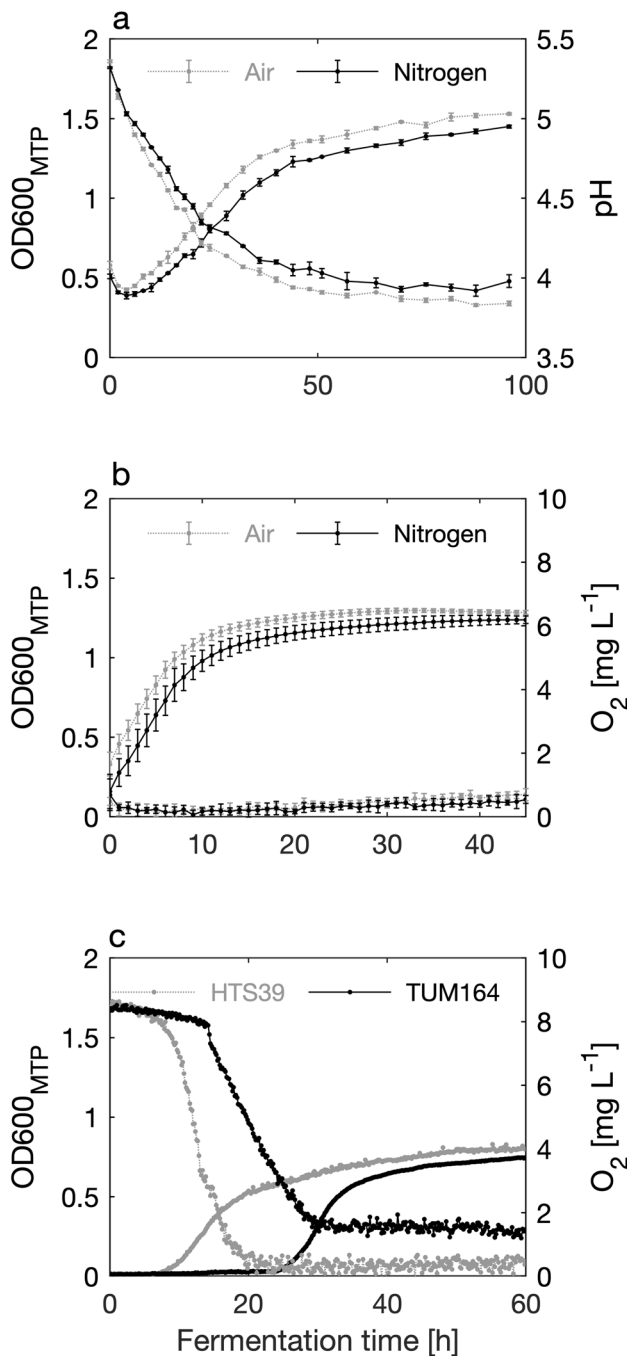


Fig. 3 Impacts of air in MTP material and headspace on beer fermentation. **a** The standard MTP material was saturated with either air or nitrogen before the 96 h fermentation of the synthetic wort by TUM34/70. The edge effect was tested by sampling at different well positions for the MTP OD600 and pH measurements at each time point. SD is visualized as error bar; **b** the OxoPlate® headspace was diffused with either air or nitrogen before the 48 h fermentation of the synthetic wort by TUM34/70; **c** two *S. pastorianus* strains HTS39 and TUM164 were monitored for their OD600 and oxygen consumption during the synthetic wort fermentation in OxoPlate®

fermentation time t (h), respectively. μ' (h^{-1}) is the apparent specific growth rate, μ (h^{-1}) is the actual specific growth rate, kd (h^{-1}) is the specific death rate, q_N (ng/cell/h) is the cell-specific sugar consumption rate, and q_P (pg/cell/h) is the cell-specific glycerol production rate.

The logistic equations, which were initially developed for the modeling of mammalian cell culture, were adopted to fit the beer fermentation for their simple scheme, robust fitting, and analytical differentiable nature [38]. The four-parameter logistic fit of the cell growth and its first-order derivation are:

$$X = \frac{A}{e^{Bt} + Ce^{-Dt}}, \quad (4)$$

$$\frac{dX}{dt} = X \left(\frac{CDe^{-Dt} - Be^{Bt}}{e^{Bt} + Ce^{-Dt}} \right), \quad (5)$$

where the viable cell density X is a nonlinear function of the fermentation time (h) and the positive parameter A , B , C and D . X is a biphasic equilibrium of both exponential growth ($X = \frac{A}{Ce^{-Dt}}$) and exponential decline ($X = \frac{A}{e^{Bt}}$). Thus, D and B are analogous to the maximum growth rate (μ_{\max}) and maximum death rate (kd_{\max}), respectively.

By setting $t = 0$ to Eq. 4, the initial cell density X_0 can be obtained as Eq. 6:

$$X_0 = \frac{A}{1 + C}. \quad (6)$$

By setting $\frac{dX}{dt} = 0$, the time required to reach the maximum cell density t_{\max} can be calculated as Eq. 7:

$$t_{\max} = \frac{\ln\left(\frac{CD}{B}\right)}{B + D}. \quad (7)$$

By substituting the t_{\max} in Eq. 4, the maximum cell density X_{\max} can be estimated by Eq. 8:

$$X_{\max} = \frac{AB}{CD\left(e^{\left(\frac{B}{B+D}\right)} + Ce^{\left(\frac{-D}{B+D}\right)}\right)}. \quad (8)$$

By substituting Eqs. 4 and 5 into Eq. 1, the apparent cell-specific growth rate μ' is available in the whole fermentation process. The maximum value μ'_{\max} can be obtained.

Initial estimates of the model parameters are essential for nonlinear regression. The initialization is typically done via the linear transformation of the nonlinear model to give starting points to the model parameters [40]. The starting points of A , B , C , and D were estimated via the linear transformation of both the exponential growth ($X = \frac{A}{Ce^{-Dt}}$) and the exponential decline ($X = \frac{A}{e^{Bt}}$) parts of Eq. 4, by fitting the measured X versus t ($t > 0$) to Eqs. 9 and 10 in the corresponding phase:

$$\ln(X) = Dt + \ln\left(\frac{A}{C}\right), \tag{9}$$

$$\ln(X) = -Bt + \ln(A). \tag{10}$$

The nutrient concentration decreases monotonically. By setting the exponential growth factor of Eq. 4 as zero ($D = 0$), the obtained equation can describe sugar consumption:

$$N = \frac{A}{e^{Bt} + C}, \tag{11}$$

$$\frac{dN}{dt} = -NB\left(1 - \frac{C}{A}N\right), \tag{12}$$

where the sugar concentration N (g/L) is a decreasing logistic function of the fermentation time t (h) and the positive parameter A , B and C . Here, B (h^{-1}) is a rate constant for the decrease of sugar concentration.

By setting $t = 0$ to Eq. 11, the initial sugar concentration N_0 can be estimated by Eq. 13. It is also the maximum sugar concentration N_{\max} in the medium.

$$N_0 = N_{\max} = \frac{A}{1 + C}. \tag{13}$$

By substituting Eqs. 4 and 12 into Eq. 2, the cell-specific sugar consumption rate q_N is available in the whole fermentation process. The maximum value $q_{N\max}$ can be obtained.

Since N_{\max} was known from the measured data, the initial estimation of A , B , and C can be obtained via the linear transformation of Eq. 11, by fitting the measured N versus t ($t > 0$) to Eq. 14:

$$\ln\left(\frac{N_{\max} - N}{N}\right) = Bt - \ln(C). \tag{14}$$

The product concentration increases monotonically. By setting the exponential decrease factor of Eq. 4 as zero ($B = 0$), the logistic increase equation can describe glycerol production:

$$P = \frac{A}{1 + Ce^{-Dt}}, \tag{15}$$

$$\frac{dP}{dt} = PD\left(1 - \frac{P}{A}\right), \tag{16}$$

where the glycerol concentration P (g/L) is an increasing logistic function of fermentation time t (h) and the non-negative constants A , B , and D . Here, D (h^{-1}) is a rate constant for the increase of glycerol concentration.

By setting $t = 0$ to Eq. 15, the initial glycerol concentration can be estimated by Eq. 17:

$$P_0 = \frac{A}{1 + C}. \tag{17}$$

By setting $\frac{dP}{dt} = 0$, the maximum glycerol concentration can be estimated by Eq. 18:

$$P_{\max} = A. \tag{18}$$

By substituting Eqs. 4 and 16 into Eq. 3, the cell-specific glycerol production rate q_P is available in the whole fermentation process. The maximum value $q_{P\max}$ can be obtained.

Since the P_{\max} can be known from the measured data, the initial estimation of A , B , and D can be obtained via the linear transformation of Eq. 15, by fitting the measured P versus t ($t > 0$) to Eq. 19:

$$\ln\left(\frac{P_{\max} - P}{P}\right) = -Dt + \ln(C). \tag{19}$$

The logistic functions (Eqs. 3, 11 and 15) were regressed independently to the mean observations. After obtaining the start points (Eqs. 9 and 10, 14, 19), two successive methods were applied to optimize the model parameters by minimizing the sum of squares error (SSE) between the experimental and the fitted data. Nonlinear least squares fitting with the trust region-reflective algorithm was firstly applied for the optimization. The resulting parameters were given as the starting points for the second-round optimization—the simplex search method in *fminsearch*. Hence, models were finalized with the parameters resulting in the lowest values of SSE. The model performance was evaluated by the coefficient (R^2) and the root-mean-square error (RMSE) of the regression.

$$R^2 = \frac{\sum_{i=1}^n (\hat{y}_i - \bar{y})^2}{\sum_{i=1}^n (y_i - \bar{y})^2}, \tag{20}$$

$$\text{RMSE} = \sqrt{\frac{\sum_{i=1}^n (y_i - \hat{y}_i)^2}{n}}, \tag{21}$$

where y is the measured data; \hat{y} , predicted value; \bar{y} , the mean of the observations; n , data density.

One-way ANOVA, followed by Tukey's pair comparison test, was performed to evaluate the significance of difference ($p < 0.05$) of the fermentation performances in MTPs, SF, and EBC. Specifically, the ANOVA was applied to live cell numbers, sugar consumption, glycerol concentration, pH, and ICP value in the time course of 192 h; to the flavor metabolites at 144 h; and to the MTP OD600, pH, and dissolved oxygen in the air references and N_2 controls, as well as to that of the two different strains. All computations were performed in MATLAB (R2020a, Mathworks, USA).

Table 2 Logistic fit parameter of beer fermentation in MTPs, SF, and EBC tube

Parameter	<i>(S. pastorianus</i> TUM34/70)					<i>(S. pastorianus</i> TUM128)				
	N0.2	S0.2	N2	SF	EBC	N0.2	S0.2	N2	SF	EBC
Live cell number										
R^2	0.98	0.99	0.995	0.99	0.97	0.95	0.95	0.90	0.99	0.92
RMSE	5.48	4.38	2.76	5.21	1.14	8.95	10.28	12.14	5.41	1.88
A	268.17	251.96	358.91	572.86	78.26	156.33	215.13	330.42	6475.12	107.58
B (kd_{\max}) [h^{-1}]	0.01	0.004	0.01	0.01	0.01	0.002	0.003	0.01	0.03	0.01
C	18.78	14.11	22.95	43.29	4.57	13.79	11.57	18.27	349.56	6.02
D (μ_{\max}) [h^{-1}]	0.05	0.05	0.04	0.04	0.03	0.07	0.05	0.04	0.03	0.02
X_{\max} [10^6 cells/mL]	148.48	160.11	138.28	162.30	33.80	126.63	153.53	127.85	168.56	32.63
t_{\max} [h]	90	101	104	113	83	88	101	100	115	82
μ'_{\max} [h^{-1}]	0.05	0.04	0.04	0.04	0.02	0.06	0.05	0.03	0.03	0.02
Sugar consumption										
R^2	0.998	0.998	0.998	0.99	0.99	0.997	0.998	0.998	1.000	0.99
RMSE	1.50	1.38	1.48	2.60	4.06	2.05	1.67	1.66	0.73	3.93
A	122.40	146.83	114.45	114.02	419.00	243.08	333.70	263.42	194.13	4099.10
B [h^{-1}]	0.04	0.05	0.04	0.04	0.02	0.04	0.06	0.05	0.05	0.06
C	0.07	0.28	0.00	0.00	2.60	1.12	1.91	1.30	0.69	35.26
$q_{N_{\max}}$ [ng/cell/h]	0.33	0.30	0.28	0.34	0.19	0.46	0.37	0.31	0.27	0.40
Glycerol concentration										
R^2	0.98	0.998	0.92	0.95	0.98	0.93	0.92	0.94	0.95	0.98
RMSE	0.05	0.02	0.11	0.09	0.05	0.16	0.15	0.15	0.09	0.07
A	1.31	1.27	1.20	1.32	1.26	1.91	1.64	1.81	1.38	1.62
C	11.41	18.31	19.09	4.92	6.92	5.94	6.27	6.19	6.60	7.50
D [h^{-1}]	0.12	0.14	0.14	0.05	0.04	0.06	0.07	0.06	0.08	0.04
P_{\max} [g/L]	1.31	1.27	1.20	1.32	1.26	1.91	1.64	1.81	1.38	1.61
$q_{P_{\max}}$ [10^{-3} pg/cell/h]	1.27	1.26	1.55	0.68	0.49	1.19	0.77	0.72	0.90	0.47

N0.2 0.2 mL static fermentation in 96 standard MTP, S0.2 0.2 mL shaking fermentation in 96 standard MTP, N2 2 mL static fermentation in 24 standard MTP, SF 200 mL shaking fermentation in 300 mL Erlenmeyer flask, EBC 2 L static fermentation in the EBC tall tube

Results

Fermentation development and kinetics

The changes in live cell numbers (LCN), sugar, and glycerol concentrations were depicted for the beer fermentation by TUM34/70 and TUM128 in MTPs, SF, and EBC tube (Fig. 1a and b). Yeast showed different patterns of LCN development at various scales at different growth phases. At the exponential growth phase, the 0.2 mL culture in 96-well MTP at static (N0.2) and shaking (S0.2) resulted in higher LCN than that of the 2 mL in the static 24-well MTP (N2) and 200 mL in the SF. The LCN of N0.2 was significantly higher than N2 at 48 h, yet the differences were insignificant at later stages of fermentation. N0.2 and S0.2 shared ($p \geq 0.05$) the exponential growth, but S0.2 reached and sustained significantly higher LCNs than N0.2 at the later stages for both the strains. The LCN of SF was similar to that in N2 at the exponential phase. Nevertheless, SF achieved the highest level of LCN as in S0.2, which were

167–170 million cells/mL for TUM34/70 and 170–175 million cells/mL for TUM128. SF decayed rapidly after 120 h in a unique pattern. The LCN of EBC was substantially lower ($p < 0.01$) than the rest scales. Different sampling, by which the suspended cells were counted in the EBC while the total cells were counted in the other scales, accounts primarily for such variances. The suspended LCN increased to the peak at 34–35 million cells/mL in 72 h and decreased gradually to 15–18 million cells/mL for both the strains.

The kinetic analysis of the mean LCN confirmed the cell growth patterns in different vessels (Table 2). The logistic fit of LCN (Eq. 4) was $R^2 \geq 0.97$, yet $RMSE \leq 5.48$ for TUM34/70, and $R^2 \geq 0.90$, yet $RMSE \leq 12.14$ for TUM128. N0.2 and N2 led to a similar level of the maximum LCNs (X_{\max}), but the former required less time to reach the peak (t_{\max}); N0.2 and S0.2 generated higher maximum growth rate (μ_{\max}) than the rest scales; S0.2 and SF reached the highest level of X_{\max} , yet the latter required longer t_{\max} . N0.2 and EBC gave the highest and the lowest μ_{\max} , which were 0.05 versus 0.03 h^{-1} for TUM34/70 and 0.07 versus 0.02 h^{-1}

for TUM128. For the strain-wise comparison, TUM34/70 generally yielded insignificantly higher LCN than TUM128 during the fermentation by all the scales.

Consistent with biomass development, rapid sugar consumption was observed in MTPs and SF (Fig. 1c and d). Wort sugars were all less than 1 g/L until 120 h. 53–71 g/L sugar was consumed within the first 24 h in MTPs in contrast to 11–17 g/L of sugar consumption in the EBC tube. TUM34/70 consumed sugar similarly in the benchtop scales (MTPs and SF). TUM128 consumed sugar faster in S0.2 than in N0.2, but only significantly at 72 h. In comparison, sugar consumption in EBC was substantially slower than the rest scales. The logistic fit of sugar consumption (Eq. 11) was $R^2 \geq 0.99$, yet $RMSE \leq 4.06$ for both strains (Table 2). The maximum sugar consumption rate ($q_{N_{max}}$) of N0.2 was higher than that in S0.2, where both were higher than N2. Compared to other scales, fermentation in SF resulted in the highest $q_{N_{max}}$ at 0.34 ng/cell/h by TUM34/70, while the lowest at 0.27 ng/cell/h by TUM128. TUM34/70 consumed sugar faster than TUM128 in MTPs and SF, but not in the EBC tube.

The two strains responded differently to the scales for glycerol accumulation (Fig. 1e and f). TUM34/70 produced about 1.3 g/L glycerol extracellularly. The accumulation was significantly faster in MTPs than SF and EBC tube. In contrast, TUM128 obtained the highest glycerol in N0.2 and N2 at 2.0 g/L, followed by S0.2 at 1.8 g/L, EBC at 1.6 g/L, and SF at 1.5 g/L. Glycerol accumulation was similar at the growth phase in all the MTPs, with a few exceptions for each strain. The logistic fit of glycerol concentration (Eq. 15) was $R^2 \geq 0.92$, yet $RMSE \leq 0.16$ for both strains. The pattern of the maximum cell-specific glycerol production rate ($q_{P_{max}}$) was different in responding to the scales between the strains (Table 2). The $q_{P_{max}}$ of TUM34/70, ranging from 0.0013 to 0.0016 pg/cell/h in MTPs, almost doubled in SF and tripled in EBC. In contrast, the $q_{P_{max}}$ of TUM128 obtained the highest at 0.0012 pg/cell/h in N0.2, followed by SF, S0.2, N2, and EBC from 0.0009 to 0.0005 pg/cell/h. TUM128 produced substantially higher ($p < 0.01$) glycerol than TUM34/70 in MTPs and EBC tube. The strains difference in glycerol yield was insignificant in SF.

Changes in the extracellular and intracellular pH

Medium pH declined fast during fermentation in the MTPs and SF for the two lager strains (Fig. 2a and b). It dropped from 5.2 to 4–4.3 by 24 h, where S0.2 was lower than N0.2 than N2 and SF for both the strains. pH in MTP and SF ranged from 3.7 to 4 at 192 h fermentation. In EBC, the pH value decreased from 5.2 to 4.8 and dropped gradually to 4.3 until 192 h. TUM34/70 resulted in significantly lower medium pH than TUM128 in MTPs and SF during fermentation.

Intracellular pH value (ICP) was sorted into three classes for the vitality evaluation in the brewing environment: very good (> 5.8), good (5.4–5.8), and bad (< 5.4) [35]. In MTPs and SF, the fermentations were initiated with bad vital cells, ICP at 5.3 for both strains (Fig. 2c and d). The yeast cells vitalized rapidly in the exponential growth phase, raising the ICP value to 5.6–5.7 in 72 h. The vitality was sustained well and declined only slightly toward the end of the fermentations. MTPs led to higher ICP than SF, significantly at the declining phase. N0.2 had higher ICP than N2, but the difference was only significant at 48 and 72 h for TUM34/70. S0.2 and N0.2 had similar ICP values during the fermentation for both strains. The cell vitality in EBC showed a different pattern. EBC fermentation was pitched with the “good” cells, ICP at 5.4 by TUM34/70 and ICP at 5.5 by TUM128. The suspended cells in EBC vitalized relatively slowly to the milliliter scales, but remained ICP above 5.8 until 192 h. ICP values were similar at 24 h in all vessels despite differences at pitching and sampling. The microscale fermentations even led to higher ICP than the rest at 48 h. The strain difference in ICP remained mostly insignificant despite the significant difference at the pitching.

Profiles of the analytical flavor

Beer flavors varied after 144 h of the undisrupted fermentations concerning scale, shaking, and MTP cover (Table 1). Anchoring to the EBC, fermentation in MTPs and SF generated similar to higher volatile metabolites with a few exceptions. The MTPs resulted in similar alcohol (by EBC at 4.0 vol%), 1.5- to 3.2-fold acetaldehyde (9 mg/L), 1- to 1.7-fold diacetyl (0.7 mg/L), 0.9- to 1.4-fold 2,3-pentandion (0.54 mg/L), more than 1.5-fold total fusel alcohols (37 mg/L), yet less than half the amount of the total detectable esters (15.6 mg/L). The direct downscaling from N2 to N0.2 resulted in substantially higher propanol, yet lower ethyl acetate ($p < 0.01$). Shaking MTP, by comparing S0.2 to N0.2, reduced propanol significantly. Besides, the gas-permeable sealed N0.2 compared to the airtight sealed A0.2 resulted in significantly higher acetaldehyde and propanol, but significantly lower diacetyl and ethyl acetate. SF yielded the highest acetaldehyde at 59 mg/L and 2-methyl butanol at 29 mg/L, but the lowest isoamyl alcohol at 4 mg/L among all the investigations. The rest of the secondary metabolites of SF were in the concentration range of MTPs.

MTP air accesses and oxygen consumption

The air accesses in the sealed MTP, via polystyrene and headspace, were evaluated for their impacts on the beer fermentation (Fig. 3a and b). Though final fermentation parameters, except for FAN, were barely changed by replacing the

cover from gas-permeable to airtight seal (Table 1), the MTP OD600 reduced significantly by excluding the air in either the MTP material or the headspace (Fig. 3a and b). When the pitching rate was 15 million live cells/mL, the dissolved oxygen was almost non-detectable in the OxoPlate®. By a single colony inoculation, *S. pastorianus* strains displayed different patterns of oxygen consumption. One lager strain (HTS39) has a short lag phase for oxygen consumption. It consumed much faster and more completely than another (TUM 164). HTS39 consumed oxygen vigorously at the exponential growth phase, which seems to be synchronized with biomass development. In comparison, TUM164 took up about 70% of the dissolved oxygen before the exponential growth (Fig. 3c).

Peripheral wells in MTP had higher risks of air diffusion and evaporation than center wells. This phenomenon is known as the edge effect, which affects the reproductivity from well-to-well of the cell-based assay [32]. As illustrated as the error bar in Fig. 3a, the variation coefficients (CVs) were all below 5% except one at 5.4% for the MTP OD600 and pH values in three different well positions at each time point during fermentation.

Discussions

MTP was considered a mature alternative to the shaking flask (SF) for many aerobic cultivations [5]. MTP (breathable membrane covered) and SF (air-tight sealed) led to indistinguishable fermentation performances for the semi-anaerobic wine fermentation. Nonetheless, lower biomass, less sugar consumption, and reduced ethanol and glycerol concentration were observed in the MTP and the SF compared with a cotton-plugged shaking flask. However, in the same MTP configuration, we observed rapid beer fermentation. Beer fermentation in these MTPs were similar to that in SF covered with aluminum foil, but both were much faster than that in the EBC tube. MTP configurations in terms of scale, shaking, and cover influenced fermentation progress, yeast physiology, and beer flavor.

Impacts of MTP configurations on beer fermentation

Industrial beer fermenters provide a natural anaerobic atmosphere for their low surface area to volume ratio [41]. The EBC tube is considered sufficient to mimic the beer production vessel by stimulating the hydrostatic pressure, natural circulation, and sedimentation to the yeast cells with the long liquid column [28, 42]. Generally, the aerated wort was the primary, often the sole, oxygen accessible to yeast cells in industrial fermentations. The dissolved oxygen was quickly consumed up within hours, primarily for the biosynthesis

of sterols and unsaturated fatty acids for cell regeneration [24]. In this scenario, slow fermentation was carried out by the suspended cells, as observed in the EBC tube. In contrast, the SF and MTPs accelerated microbial reproduction, sugar consumption, and glycerol accumulation of the beer fermentation. These benchtop fermenters are more susceptible to the presence of environmental oxygen when handling at smaller volumes. Though the wort-dissolved oxygen was rapidly consumed up in the MTP (Fig. 3b and c), the micro-culture in the MTP well was still surrounded by air, namely, the air from the headspace via relative large contacting surface [5], from the oxygenated well surface of the cell culture plate [12], and via the air-saturated plastic material during the fermentation [20, 21]. Under certain conditions, *S. cerevisiae* could change the fermentation into the mixed respire-fermentation, characterized by the operation of the tricarboxylic acid (TCA) cycle and the activation of NADH shuttles from the cytosol to mitochondria [43]. However, beer fermentation is dominated by the Crabtree effect. An initial glucose concentration above 0.15 g/L would set the glycolytic flow toward ethanol even in the presence of oxygen [44]. Though the excessive air supply in MTPs and SF did not change the alcoholic fermentation, it did stimulate yeast growth and sugar consumption [24]. Hence, the high cell numbers and rapid sugar consumption in MTPs could be attributed to the higher static OTR by the miniaturization.

Shaking MTP did not further enhance the growth rate and sugar consumption at the exponential growth phase. Indeed, the maximum OTR remained constant at the static level by up to 450 rpm shaking of the 96 standard MTP [13, 14]. A stagnant layer of cells rapidly formed at the bottom of MTP. Even visible movement of the culture was observed by 300 rpm shaking (data not shown). Both TUM34/70 and TUM128 are flocculating yeast strains, which means they tend to form agglutinate clumps and settle at the bottom during fermentation compared to their less flocculating peers [31]. Adding to the biological factor, the dimensional miniaturization of MTP further enhanced yeast cell sedimentation. CO₂ bubbling, which spontaneously initiates the fluid motion [27], is shorted in its path length and reduced in its quantity in the microliter fermentation. Shear rate, of which a minimum value was required to keep the cell in suspension [28, 29], drops with the reduction in the liquid height. Surface tension, which counteracts the liquid flow and movement, the counteracting effect was enhanced in vessels with less than 8 mm diameter. These factors could have contributed to the early and quick sedimentation of the *S. pastorianus* cells in the MTPs. Nevertheless, early sedimentation did not cause stagnant fermentation in MTPs. It is potentially due to the following reasons. Firstly, microwell enables relatively large cell-liquid contacting surface even with the bottom layer of cells settlements. Secondly, the increased fermentation rate in MTPs led to faster CO₂ generation. The

bubbling drove the shear rate up and kept sufficient cells in suspension at the early stage of fermentation [28]. We observed that the shaking MTP yielded and sustained higher live cell numbers than the static MTP. The high cell numbers could be attributed to the improving shaking efficiency with time, in addition to the potential respire–fermentative growth [43]. The higher air–liquid contacting surface could have occurred with the lower wetting tension caused by the biosurfactant accumulation (such as cell membrane components, proteins, and extracellular glycolipid in biomass) even at the same shaking frequency [13]. Notice that the dynamic viscosity increased as well with biomass. The OTR decreased as the medium viscosity increased [45]. However, viscosity by up to 35 mPa s did not impact OTR and the mixing in the microbioreactor fermentation [46].

To the apex of glycerol concentration, MTPs shortened the fermentation time by half compared to the EBC fermentation by TUM34/70. The primary physiological roles of glycerol biosynthesis indicate the rapid glycerol accumulation. By maintaining the cytosolic redox balance, the ‘redox sink’ glycerol was formed to oxidize the surplus NADH during anaerobic growth [47]. Over 60% of the total NADH was estimated from biomass production [48, 49]. By confronting the hyperosmotic environment, the ‘osmolyte’ glycerol was induced as the primary compatible solute to sustain the intracellular turgor [50]. Thus, rapid glycerol accumulation was consistent with rapid biomass development and sugar consumption, as seen in MTPs. The shaking MTP generated less glycerol than the static MTP, but the extent of reduction depended on the strains (Fig. 1e and f). Additionally, the airtight sealing yielded higher glycerol than gas-permeable sealing (Table 1). These observations confirmed the negative role of oxygen in glycerol formation. Anaerobiosis upregulated the expression of *GPD2* and *GPP1* in glycerol biosynthesis [51]. With the increasing level of dissolved oxygen, the cytosolic NADH/NAD⁺ ratio increased, but glycerol decreased over the mitochondrial oxidization of NADH in the respire–fermentation [43, 52]. Despite that, several studies have found that agitation rarely or slightly increased the glycerol in wine fermentations [10, 26, 53]. Indeed, the metabolic reaction toward oxygen was strain dependent [24]. As in this study, relative to TUM34/70, TUM128 was more susceptible to the scale and shaking concerning glycerol production. Potentially, it was due to their different response to the oxygen during fermentation. Lager strains showed different patterns of oxygen consumption. Not only the absolute amount, but also absorption time, rate, and the correlation to cell reproduction were different among the lager brewing strains (Fig. 3c).

Impacts of MTP configurations on the cell growth

The vital cell pumps protons continuously against a gradient from the cytosol to the extracellular medium to maintain the

optimum neutral range of pH for the metabolic reactions (54). Rapid medium acidification—pH dropped from 5.2 to 4 in 48 h, and simultaneous cell vitalization—ICP increased from 5.3 to 5.6, were observed in the growth phase of MTP fermentations (Fig. 2). The low extracellular pH in MTPs and SF could be explained by the production of organic acids and the formation of carbonic acid from the dissolved CO₂ adding to the proton transportation [55]. At the early stage, the yeast cells were supplied with sufficient nutrients and oxygen. Both contributed to the physiological health of the cells [56, 57]. With the proceeding of fermentation, the extracellular environment deteriorated with the depletion of nutrients and the simultaneous accumulation of pro-aging metabolites such as ethanol and organic acids. Such environmental changes harmed cell vitality [58, 59]. Compared to the anaerobic culture, aerobic culture improved the cell viability, stress resistance, and chronological life span of *S. cerevisiae* in the stationary phase [41, 60]. Aligned with these researches, the shaking MTP had higher ICP at the later stage of fermentation (Fig. 2a and b). The necessary correlations from oxygen availability to oxidative stress were still arguable in brewing conditions [57, 61]. The oxidative stress-responsive genes were overexpressed in the 51.8 ppm oxygenated wort. However, it did not affect the cell viability of the high-density yeast population [57]. The dimensional miniaturization has been long presumed to have little effect on the individual cell physiology. It was argued that the diameter of a standard 96 MTP (Ø 0.64 cm) is still a factor of 10³ larger than that of the average yeast cell (Ø 5 µm) [5]. Hereby, we provided concrete evidence by flow cytometry technology. The MTP miniaturization did not hinder individual cell vitality in terms of ICP. It is even beneficial to rapid cell vitalization during beer fermentation by *S. pastorianus* strains.

Impacts of MTP configurations on beer flavor

Acetaldehyde conveys grassy off-flavor with a threshold at about 10 mg/L in beer [55]. Except for the airtight sealed MTP (A0.2), the rest of the MTPs and SF have at least double the amount of acetaldehyde from EBC fermentation (Table 1). The rapid growth in SF and MTPs inevitably led to high acetaldehyde concentrations—the direct precursor of ethanol formation in alcoholic fermentation. The early sedimentation of cells in MTPs could have hindered the re-utilization of the excreted acetaldehyde [62]. What is more, cell autolysis, especially in SF at the late stage of fermentation (Fig. 1a and b), could have released a large amount of acetaldehyde and led to the highest level at 59 mg/L. Oxygenation stimulated acetaldehyde production in continuous beer fermentation [63], but a lower concentration was obtained from the batch fermentation with higher initial dissolved oxygen [25]. Additionally, ethanol could have been oxidized back

to acetaldehyde through the diauxic shift effect considering the rapid sugar depletion and the potential air accesses in MTPs and SF [61, 64].

Vicinal diketones (VDK), including diacetyl with a threshold at 0.15 mg/L and 2,3-pentanedione at 0.9 mg/L, exert butter-like flavors to beers [65]. A0.2 and N2 fermentation resulted in significantly higher diacetyl (1.1–1.2 mg/L) than the rest scales (0.7–0.8 mg/L). Such observation could be attributed to the dynamics between diacetyl formation and reduction during the lager yeast fermentation. Diacetyl is formed by spontaneous non-enzymatic oxidative decarboxylation of α -acetolactate that is intermediate of the valine biosynthesis pathway [62]. Conditions allowing more valine biosynthesis or favoring rapid yeast growth give more diacetyl formation at the early growth phase [65]. Diacetyl can be re-assimilated and further reduced into 2,3-butanediol via acetoin under several ketone reductases at the later fermentation stage. Factors influencing cell membrane compositions and yeast behaviors in flocculation and sedimentation also affected diacetyl removal efficiency [65]. MTP scale miniaturization (compare N0.2 to N2) enhanced the maximum growth rate (Table 2), yet yielded significantly lower diacetyl (Table 1). MTP shaking (compare S0.2 to N0.2) obtained higher cell numbers (Fig. 1), yet resulted in slightly lower diacetyl (Table 1). Scale miniaturization, shaking, and gas-permeable sealing all have intrinsic higher OTR, which favors α -acetolactate oxidization, and consequently diacetyl formation. However, lower diacetyl was observed in these conditions. It might be due to the active removal at the later fermentation stage, considering that higher cell vitality (ICP) was obtained in the MTPs featuring scale miniaturization, shaking, and gas-permeable sealing (Fig. 1 and Table 1). Additionally, an acidic environment was in favor of both diacetyl formation and reduction [62]. The MTP scale miniaturization and shaking also resulted in lower medium pH during the fermentation process.

Higher alcohols and esters deliver a broad spectrum of fruity aromas to beer [55]. The MTPs and SF fermentations resulted in significantly higher fusel alcohols, yet lower ester concentration than EBC (Table 1). Oxygen favored higher alcohol but not ester formation [25, 26, 57], though with exceptions [26, 66]. In the MTPs and SF environment, oxygen stimulated biomass accumulation, which could be the primary reason for their higher fusel alcohol yield. Meanwhile, oxygen inhibited the genes involved in ester formation and resulted in lower and fewer esters [57, 67]. Notice that fermentation in SF resulted in the highest level of biomass and acetaldehyde, yet the lowest level of alcohol and glycerol, which were on the opposites in EBC. Depending on the configurations, MTPs obtained in-between levels of these attributes. The airtight cover pulled glycerol, acetaldehyde, most higher alcohols, and esters closer to that in the EBC fermentation (Table 1). The interaction between yeast cells

and its unique fermentation environment, especially concerning the potential air supply, might be the primary reason for the unique flavor patterns.

Impacts of limiting air access in MTP on beer fermentation

The material of the applied MTP covers differs in air permeability. The MTP cover made of the relative gas-permeable polyurethane significantly elevated the maximum oxygen transfer capacity than that of the comparable airtight polyester [16]. However, the gas-permeable cover only slightly enhanced the beer fermentation (Table 1). The insignificance could be partly caused by the inadequate air permeability of the applied ‘gas-permeable’ seal [16, 17]. Furthermore, the produced CO₂ in the sealed MTP well could have stratified to form a layer beneath air to prevent further air–liquid surface contact in the headspace. The MTP covers bumped up at each well during the exponential growth phase, and the gas-permeable cover concaved later toward the end of the wort fermentation (data not shown). This observation indicated the potential impacts of CO₂ withheld in the sealed MTP during alcoholic fermentation. Intuitively, in the airtight sealed MTP, cells could have experienced higher in-well pressure than the gas-permeable covered MTP because of the entrapped CO₂ at the early fermentation stage. Higher top pressure and dissolved CO₂ reduced not only the fermentation activity and cell vitality [68, 69], but also changed the flavor profile [34, 70, 71]. Endogenous CO₂ could have influenced the fermentation and flavor profile in different MTP configurations. Noticeably, the changed plasticity of the gas-permeable seal indicated potential air diffusion upon atmosphere pressure and highlighted the risks of contamination and evaporation. Hence, the relatively rigid airtight seal performed better by slowing down the beer fermentation and balancing the flavor profile.

Besides, MTP cover is universally required to ensure well-to-well equalization [5]. By sealing the MTP with the airtight seal, less than five CV% were detected for both the MTP OD600 and pH in different peripheral and center wells (Fig. 3a). It suggested a very good well-to-well reproducibility, yet minimum edge effect of the standard MTP for the beer fermentation. None of the blank controls (synthetic wort medium) got contaminated when each was surrounded by individual fermentations (data not shown). The airtight seal further proved its effectiveness in preventing well-to-well cross-contamination. Evaporation is a central issue of MTP-based cultivations. Low evaporation rate was expected in the MTP lager beer fermentation considering the low fermentation temperature (12 °C), the humidity control (70%), the airtight cover, and what is more the low evaporation rate observed in similar configurations [6, 10].

Polystyrene MTP is oxygen permeable. Significant oxygen diffusion was observed from polystyrene MTP to the

culture medium [20]. As the depletion of wort dissolved oxygen, the oxygen probably diffused into the wort and stimulated the fermentation. It could explain the significantly lower fermentative activities of TUM34/70 by excluding the air in the MTP material (Fig. 3a). However, oxygen consumption was barely detectable at the pitching rate of 15 million cells/mL at room temperature fermentation (Fig. 3b). The rapid cell sedimentation due to the biological and dimensional factors could have biased the OxoPlate® measurement, adding to the relatively high pitching rate and the intrinsic uneven distribution of the dissolved oxygen in MTP well [20, 21]. Oxygen exchange happened predominantly via the medium and air interface in the sealed MTP [20]. By filling the headspace with N₂, the yeast growth reduced significantly in the microwell fermentation (Fig. 3b). However, pitching in the air cast significantly higher initial MTP OD600 than pitching in the anaerobic box. Other than the headspace gas, the significant differentiation of cell growth could have been caused by the initial difference. Such a difference further highlighted the impacts of environmental air in handling the micro-volume in the anaerobic fermentation.

This study has several limitations, firstly the sampling methods. To resolve the conflicts between minimized MTP culture and the analytical requirement, we collected samples in each column or each MTP to represent what has happened in the individual well. Though little variance was detected at different well positions (Fig. 3a), the “average then out” strategy and the sampling operation such as in-well mixing could have influenced the analytical value at each representing time point. Additionally, the shaking flask fermentation was disturbed by the handshaking homogenization and by pulling samples out for analysis at each time point. Such operations introduced not only air, but also potential variances. However, the end-point analysis of the undisrupted fermentations (Table 1) confirmed our observations in the time series (Figs. 1 and 2). Secondly, with regard to the different batches, yeast strains went through the same propagation procedure and in the same fermentation parameter. However, the EBC was based on separate batches from the MTPs and SF (Figs. 1 and 2). The cell analysis of the former was assayed on the suspended cells, while the latter was assayed on the total cells. Additionally, a different medium and two different MTPs were adopted to evaluate the impacts of material and headspace air on the fermentation (Fig. 3). Thus, sampling and batches could have introduced variations.

Conclusion

The high static OTR of MTP, which has been advantageous for aerobic cultivation, accelerated *S. Pastorianus* fermentation and changed the beer flavor, hence affecting the scalability of MTP in anaerobic fermentations. The scale, shaking,

and cover of MTP influenced beer fermentation differently. The downscaling accelerated the yeast reproduction and vitalization; the shaking MTP reached and sustained higher live cell numbers, and the adhesive covers impacted mainly the flavor metabolites. These influences were partly attributed to air access in MTP fermentation. Future efforts are expected to improve the scalability of the MTP anaerobic cultivations. First is to restrict air access in MTP configurations. Beer fermentation was slowed down by excluding air in the MTP material and headspace. Previous efforts that aimed at increasing OTR for aerobic fermentation could be reversely applied for the anaerobic fermentation. The shape, material, surface treatment, filling volume, and cover design of MTPs has to be customized for anaerobic applications. Notice that the place-in-anaerobicity strategy was direct and effective for creating an anaerobic environment. However, alternative solutions are critical for the flexible automation of the MTP-based HTS applications. Second is to address the endogenous carbon dioxide in sealed MTP. The released CO₂ pressurized MTP covers during the beer fermentation and the gas-permeable cover changed its shape and texture correspondingly. As revealed in the sealed system for wine fermentation, the endogenous CO₂ changed the process parameters such as headspace pressure and dissolved CO₂. It impacted yeast stress responses, metabolites, and organoleptic properties of wine [34, 72]. Since little is known on the impacts of endogenous CO₂ in sealed MTPs, further clarifications are desired. Last but not least, yeast strains responded differently to MTP miniaturization. In the case of glycerol yield, TUM34/70 produced the same amount at different scales, yet TUM128 quickly produced more in MTPs. The accelerated glycerol production can further enhance the high-throughput capacity of MTP fermentation by reducing the recycling time. However, careful interpretation and verification of the screening results are required. This study aids the interpretation of the beverage fermentation in standard MTPs and provides insights into the scalability of MTP-based HTS in the anaerobic cultivations.

Acknowledgements The authors thank the China Scholarship Council for providing scholarship under grant number No. 201206320112.

Funding Open Access funding enabled and organized by Projekt DEAL.

Declarations

Conflict of interest The authors declare no conflict of interest.

Compliance with ethics requirements The authors declare compliance with ethics requirements.

Open Access This article is licensed under a Creative Commons Attribution 4.0 International License, which permits use, sharing, adaptation, distribution and reproduction in any medium or format, as long

as you give appropriate credit to the original author(s) and the source, provide a link to the Creative Commons licence, and indicate if changes were made. The images or other third party material in this article are included in the article's Creative Commons licence, unless indicated otherwise in a credit line to the material. If material is not included in the article's Creative Commons licence and your intended use is not permitted by statutory regulation or exceeds the permitted use, you will need to obtain permission directly from the copyright holder. To view a copy of this licence, visit <http://creativecommons.org/licenses/by/4.0/>.

References

- Back A, Rossignol T, Krier F, Nicaud JM, Dhulster P (2016) High-throughput fermentation screening for the yeast *Yarrowia lipolytica* with real-time monitoring of biomass and lipid production. *Microb Cell Fact* 15:147. <https://doi.org/10.1186/s12934-016-0546-z>
- Lv X, Song J, Yu B, Liu H, Li C, Zhuang Y, Wang Y (2016) High-throughput system for screening of high L-lactic acid-productivity strains in deep-well microtiter plates. *Bioprocess Biosyst Eng* 39:1737–1747. <https://doi.org/10.1007/s00449-016-1649-y>
- Wewetzer SJ, Kunze M, Ladner T, Luchterhand B, Roth S, Rahmen N, Kloss R, Costa ESA, Regestein L, Buchs J (2015) Parallel use of shake flask and microtiter plate online measuring devices (RAMOS and BioLector) reduces the number of experiments in laboratory-scale stirred tank bioreactors. *J Biol Eng* 9:9. <https://doi.org/10.1186/s13036-015-0005-0>
- Isett K, George H, Herber W, Amanullah A (2007) Twenty-four-well plate miniature bioreactor high-throughput system: assessment for microbial cultivations. *Biotechnol Bioeng* 98:1017–1028. <https://doi.org/10.1002/bit.21484>
- Duetz WA (2007) Microtiter plates as mini-bioreactors: miniaturization of fermentation methods. *Trends Microbiol* 15:469–475. <https://doi.org/10.1016/j.tim.2007.09.004>
- Hevekerl A, Kuenz A, Vorlop KD (2014) Filamentous fungi in microtiter plates—an easy way to optimize itaconic acid production with *Aspergillus terreus*. *Appl Microbiol Biotechnol* 98:6983–6989. <https://doi.org/10.1007/s00253-014-5743-2>
- Kensy F, Engelbrecht C, Buchs J (2009) Scale-up from microtiter plate to laboratory fermenter: evaluation by online monitoring techniques of growth and protein expression in *Escherichia coli* and *Hansenula polymorpha* fermentations. *Microb Cell Fact* 8:68. <https://doi.org/10.1186/1475-2859-8-68>
- Van Renterghem L, Clicque H, Huyst A, Roelants S, Soetaert W (2019) Miniaturization of *Starmerella bombicola* fermentation for evaluation and increasing (novel) glycolipid production. *Appl Microbiol Biotechnol* 103:4347–4362. <https://doi.org/10.1007/s00253-019-09766-3>
- Kosa G, Vuoristo KS, Horn SJ, Zimmermann B, Afseth NK, Kohler A, Shapaval V (2018) Assessment of the scalability of a microtiter plate system for screening of oleaginous microorganisms. *Appl Microbiol Biotechnol* 102:4915–4925. <https://doi.org/10.1007/s00253-018-8920-x>
- Liccioli T, Tran TM, Cozzolino D, Jiranek V, Chambers PJ, Schmidt SA (2011) Microvinification—how small can we go? *Appl Microbiol Biotechnol* 89:1621–1628. <https://doi.org/10.1007/s00253-010-2992-6>
- Lattermann C, Funke M, Hansen S, Diederichs S, Buchs J (2014) Cross-section perimeter is a suitable parameter to describe the effects of different baffle geometries in shaken microtiter plates. *J Biol Eng* 8:18. <https://doi.org/10.1186/1754-1611-8-18>
- Lerman MJ, Lembong J, Muramoto S, Gillen G, Fisher JP (2018) The evolution of polystyrene as a cell culture material. *Tissue Eng Part B Rev* 24:359–372. <https://doi.org/10.1089/ten.TEB.2018.0056>
- Doig SD, Pickering SCR, Lye GJ, Baganz F (2005) Modelling surface aeration rates in shaken microtitre plates using dimensionless groups. *Chem Eng Sci* 60:2741–2750. <https://doi.org/10.1016/j.ces.2004.12.025>
- Hermann R, Lehmann M, Buchs J (2003) Characterization of gas-liquid mass transfer phenomena in microtiter plates. *Biotechnol Bioeng* 81:178–186. <https://doi.org/10.1002/bit.10456>
- Duetz WA, Ruedi L, Hermann R, O'Connor K, Buchs J, Witholt B (2000) Methods for intense aeration, growth, storage, and replication of bacterial strains in microtiter plates. *Appl Environ Microbiol* 66:2641–2646. <https://doi.org/10.1128/AEM.66.6.2641-2646.2000>
- Sieben M, Giese H, Grosch JH, Kauffmann K, Buchs J (2016) Permeability of currently available microtiter plate sealing tapes fail to fulfil the requirements for aerobic microbial cultivation. *Biotechnol J* 11:1525–1538. <https://doi.org/10.1002/biot.201600054>
- Zimmermann HF, John GT, Trauthwein H, Dingerdissen U, Huthmacher K (2003) Rapid evaluation of oxygen and water permeation through microplate sealing tapes. *Biotechnol Prog* 19:1061–1063. <https://doi.org/10.1021/bp025774t>
- Lam KL, Lin S, Liu C, Wu X, Tang S, Kwan HS, Cheung PC (2018) Low-cost method generating in situ anaerobic conditions on a 96-well plate for microbial fermentation in food research. *J Agric Food Chem* 66:11839–11845. <https://doi.org/10.1021/acs.jafc.8b04888>
- Kensy F (2011) Anaerobic high-throughput fermentation. *Genet Eng Biotechnol* 31:38–39. <https://doi.org/10.1089/gen.31.04.17>
- Arain S, Weiss S, Heinze E, John GT, Krause C, Klimant I (2005) Gas sensing in microplates with optodes: influence of oxygen exchange between sample, air, and plate material. *Biotechnol Bioeng* 90:271–280. <https://doi.org/10.1002/bit.20348>
- Polymeropoulos ET, Elliott NG, Wotherspoon SJ, Frappell PB (2013) Respirometry: correcting for diffusion and validating the use of plastic multiwell plates with integrated optodes. *Physiol Biochem Zool* 86:588–592. <https://doi.org/10.1086/671800>
- Pfeiffer T, Morley A (2014) An evolutionary perspective on the Crabtree effect. *Front Mol Biosci* 1:17. <https://doi.org/10.3389/fmolb.2014.00017>
- Piskur J, Rozpedowska E, Polakova S, Merico A, Compagno C (2006) How did *Saccharomyces* evolve to become a good brewer? *Trends Genet* 22:183–186. <https://doi.org/10.1016/j.tig.2006.02.002>
- Kirsop BH (1974) Oxygen in brewery fermentation. *J Inst Brew* 80:252–259. <https://doi.org/10.1002/j.2050-0416.1974.tb03614.x>
- Kucharczyk K, Tuszyński T (2017) The effect of wort aeration on fermentation, maturation and volatile components of beer produced on an industrial scale. *J Inst Brew* 123:31–38. <https://doi.org/10.1002/jib.392>
- Rollero S, Roberts S, Bauer FF, Divol B (2018) Agitation impacts fermentation performance as well as carbon and nitrogen metabolism in *Saccharomyces cerevisiae* under winemaking conditions. *Aust J Grape Wine Res* 24:360–367. <https://doi.org/10.1111/ajgw.12338>
- Delente J, Akin C, Krabbe E, Ladenburg K (1969) Fluid dynamics of anaerobic fermentation. *Biotechnol Bioeng* 11:631–646. <https://doi.org/10.1002/bit.260110410>
- Lake JC, Speers RA, Porter AV, Gill TA (2018) Miniaturizing the fermentation assay: effects of fermentor size and fermentation kinetics on detection of premature yeast flocculation. *J Am Soc Brew Chem* 66:94–102. <https://doi.org/10.1094/asbcj-2008-0213-01>
- MacIntosh AJ, Adler J, Eck E, Speers RA (2012) Suitability of the miniature fermentability method to monitor industrial

- fermentations. *J Am Soc Brew Chem* 70:205–211. <https://doi.org/10.1094/ASBCJ-2012-0724-01>
30. Vidgren V, Londesborough J (2011) 125th Anniversary review: yeast flocculation and sedimentation in brewing. *J Inst Brew* 117:475–487. <https://doi.org/10.1002/j.2050-0416.2011.tb00495.x>
 31. Narziss L, Back W, Gastl M, Zarnkow M (2017) *Abriss der Bierbrauerei*. Wiley-VCH, Weinheim
 32. Lundholt BK, Scudder KM, Pagliaro L (2003) A simple technique for reducing edge effect in cell-based assays. *J Biomol Screen* 8:566–570. <https://doi.org/10.1177/1087057103256465>
 33. Fischer S, Engstler C, Procopio S, Becker T (2016) EGFP-based evaluation of temperature inducible native promoters of industrial ale yeast by using a high throughput system. *LWT Food Sci Technol* 68:556–562. <https://doi.org/10.1016/j.lwt.2015.12.020>
 34. Li H, Su J, Ma W, Guo A, Shan Z, Wang H (2015) Metabolic flux analysis of *Saccharomyces cerevisiae* in a sealed winemaking fermentation system. *FEMS Yeast Res* 15:fou010. <https://doi.org/10.1093/femsyr/fou010>
 35. Thiele F, Back W (2005) Measurement of yeast vitality using a modified version of the intracellular pH measurement (ICP). *Monatsschr Brauwiss* 58:2–5
 36. Verma M (2013) HPAE-PAD for the analysis of carbohydrates. Thermo Fisher Scientific, Sunnyvale, CA
 37. MEBAK®, (2002) *Brautechnische Analysenmethoden Sudwerk-kontrolle, Würze, Bier*. Fachverlag Hans Carl GmbH, Freising, Biermischgetränke und AFG
 38. MEBAK®, (2006) *Brautechnische Analysenmethoden Rohstoffe*. Fachverlag Hans Carl GmbH, Freising
 39. Procopio S, Krause D, Hofmann T, Becker T (2013) Significant amino acids in aroma compound profiling during yeast fermentation analyzed by PLS regression. *LWT Food Sci Technol* 51:423–432. <https://doi.org/10.1016/j.lwt.2012.11.022>
 40. Goudar CT (2012) Analyzing the dynamics of cell growth and protein production in mammalian cell fed-batch systems using logistic equations. *J Ind Microbiol Biotechnol* 39:1061–1071. <https://doi.org/10.1007/s10295-012-1107-z>
 41. da Costa BLV, Basso TO, Raghavendran V, Gombert AK (2018) Anaerobiosis revisited: growth of *Saccharomyces cerevisiae* under extremely low oxygen availability. *Appl Microbiol Biotechnol* 102:2101–2116. <https://doi.org/10.1007/s00253-017-8732-4>
 42. Tyrell T (2012) Experiences with new fermentation test-tubes—standardized small scale fermentation from wort to bottle. World Brewing Congress, Portland, OR
 43. Aceituno FF, Orellana M, Torres J, Mendoza S, Slater AW, Melo F, Agosin E (2012) Oxygen response of the wine yeast *Saccharomyces cerevisiae* EC1118 grown under carbon-sufficient, nitrogen-limited enological conditions. *Appl Environ Microbiol* 78:8340–8352. <https://doi.org/10.1128/AEM.02305-12>
 44. Verduyn C, Zomerdijk TPL, van Dijken JP, Scheffers WA (1984) Continuous measurement of ethanol production by aerobic yeast suspensions with an enzyme electrode. *Appl Microbiol Biotechnol* 19:181–185. <https://doi.org/10.1007/bf00256451>
 45. Running JA, Bansal K (2016) Oxygen transfer rates in shaken culture vessels from Fernbach flasks to microtiter plates. *Biotechnol Bioeng* 113:1729–1735. <https://doi.org/10.1002/bit.25938>
 46. Hlaváč P, Božiková M, Cviklovič V (2016) Dynamic viscosity and activation energy of wort during fermentation and storing. *Acta Technol Agric* 19:6–9. <https://doi.org/10.1515/ata-2016-0002>
 47. Ansell R, Granath K, Hohmann S, Thevelein JM, Adler L (1997) The two isoenzymes for yeast NAD⁺-dependent glycerol 3-phosphate dehydrogenase encoded by GPD1 and GPD2 have distinct roles in osmoadaptation and redox regulation. *EMBO J* 16:2179–2187. <https://doi.org/10.1093/emboj/16.9.2179>
 48. Celton M, Goelzer A, Camarasa C, Fromion V, Dequin S (2012) A constraint-based model analysis of the metabolic consequences of increased NADPH oxidation in *Saccharomyces cerevisiae*. *Metab Eng* 14:366–379. <https://doi.org/10.1016/j.ymben.2012.03.008>
 49. Bakker BM, Overkamp KM, van Maris AJ, Kotter P, Luttk MA, van Dijken JP, Pronk JT (2001) Stoichiometry and compartmentation of NADH metabolism in *Saccharomyces cerevisiae*. *FEMS Microbiol Rev* 25:15–37. <https://doi.org/10.1111/j.1574-6976.2001.tb00570.x>
 50. Albertyn J, Hohmann S, Prior BA (1994) Characterization of the osmotic-stress response in *Saccharomyces cerevisiae*: osmotic stress and glucose repression regulate glycerol-3-phosphate dehydrogenase independently. *Curr Genet* 25:12–18. <https://doi.org/10.1007/BF00712960>
 51. Costenoble R, Valadi H, Gustafsson L, Niklasson C, Franzen CJ (2000) Microaerobic glycerol formation in *Saccharomyces cerevisiae*. *Yeast* 16:1483–1495. [https://doi.org/10.1002/1097-0061\(200012\)16:16%3c1483::AID-YEA642%3e3.0.CO;2-K](https://doi.org/10.1002/1097-0061(200012)16:16%3c1483::AID-YEA642%3e3.0.CO;2-K)
 52. Pham TH, Mauvais G, Vergoignan C, De Coninck J, Dumont F, Lherminier J, Cachon R, Feron G (2008) Gaseous environments modify physiology in the brewing yeast *Saccharomyces cerevisiae* during batch alcoholic fermentation. *J Appl Microbiol* 105:858–874. <https://doi.org/10.1111/j.1365-2672.2008.03821.x>
 53. Casalta E, Aguera E, Picou C, Rodriguez-Bencomo JJ, Salmon JM, Sablayrolles JM (2010) A comparison of laboratory and pilot-scale fermentations in winemaking conditions. *Appl Microbiol Biotechnol* 87:1665–1673. <https://doi.org/10.1007/s00253-010-2652-x>
 54. Weigert C, Steffler F, Kurz T, Shellhammer TH, Methner FJ (2009) Application of a short intracellular pH method to flow cytometry for determining *Saccharomyces cerevisiae* vitality. *Appl Environ Microbiol* 75:5615–5620. <https://doi.org/10.1128/AEM.00650-09>
 55. Briggs DE, Boulton CA, Brookes PA, Stevens R (2004) *Brewing science and practice*. Woodhead Publishing Limited, Cambridge
 56. Verbelen PJ, Depraetere SA, Winderickx J, Delvaux FR, Delvaux F (2009) The influence of yeast oxygenation prior to brewery fermentation on yeast metabolism and the oxidative stress response. *FEMS Yeast Res* 9:226–239. <https://doi.org/10.1111/j.1567-1364.2008.00476.x>
 57. Verbelen PJ, Saerens SM, Van Mulders SE, Delvaux F, Delvaux FR (2009) The role of oxygen in yeast metabolism during high cell density brewery fermentations. *Appl Microbiol Biotechnol* 82:1143–1156. <https://doi.org/10.1007/s00253-009-1909-8>
 58. Longo VD, Fabrizio P (2012) Chronological aging in *Saccharomyces cerevisiae*. *Subcell Biochem* 57:101–121. https://doi.org/10.1007/978-94-007-2561-4_5
 59. Mohammad K, Dakik P, Medkour Y, McAuley M, Mitrofanova D, Titorenko VI (2018) Some metabolites act as second messengers in yeast chronological aging. *Int J Mol Sci* 19:860–874. <https://doi.org/10.3390/ijms19030860>
 60. Bisschops MM, Vos T, Martinez-Moreno R, Cortes PT, Pronk JT, Daran-Lapujade P (2015) Oxygen availability strongly affects chronological lifespan and thermotolerance in batch cultures of *Saccharomyces cerevisiae*. *Microb Cell* 2:429–444. <https://doi.org/10.15698/mic2015.11.238>
 61. Gibson BR, Lawrence SJ, Boulton CA, Box WG, Graham NS, Linforth RS, Smart KA (2008) The oxidative stress response of a lager brewing yeast strain during industrial propagation and fermentation. *FEMS Yeast Res* 8:574–585. <https://doi.org/10.1111/j.1567-1364.2008.00371.x>
 62. Stewart G (2017) The production of secondary metabolites with flavour potential during brewing and distilling wort fermentations. *Fermentation* 3:63. <https://doi.org/10.3390/fermentation3040063>
 63. Kuriyama H, Kobayashi H (1993) Effects of oxygen supply on yeast growth and metabolism in continuous fermentation. *J Ferment Bioeng* 75:364–367. [https://doi.org/10.1016/0922-338x\(93\)90135-u](https://doi.org/10.1016/0922-338x(93)90135-u)

64. James TC, Campbell S, Donnelly D, Bond U (2003) Transcription profile of brewery yeast under fermentation conditions. *J Appl Microbiol* 94:432–448. <https://doi.org/10.1046/j.1365-2672.2003.01849.x>
65. Krogerus K, Gibson BR (2013) 125th Anniversary review: diacetyl and its control during brewery fermentation. *J Inst Brew* 119:86–97. <https://doi.org/10.1002/jib.84>
66. Espinosa Vidal E, de Morais Jr MA, Francois JM, de Billerbeck GM (2015) Biosynthesis of higher alcohol flavour compounds by the yeast *Saccharomyces cerevisiae*: impact of oxygen availability and responses to glucose pulse in minimal growth medium with leucine as sole nitrogen source. *Yeast* 32:47–56. <https://doi.org/10.1002/yea.3045>
67. Saerens SM, Delvaux FR, Verstrepen KJ, Thevelein JM (2010) Production and biological function of volatile esters in *Saccharomyces cerevisiae*. *Microb Biotechnol* 3:165–177. <https://doi.org/10.1111/j.1751-7915.2009.00106.x>
68. Dixon NM, Kell DB (1989) The inhibition by CO₂ of the growth and metabolism of micro-organisms. *J Appl Bacteriol* 67:109–136. <https://doi.org/10.1111/j.1365-2672.1989.tb03387.x>
69. Kruger L, Pickerell ATW, Axcell B (1992) The sensitivity of different brewing yeast strains to carbon dioxide inhibition: fermentation and production of flavour-active volatile compounds. *J Inst Brew* 98:133–138. <https://doi.org/10.1002/j.2050-0416.1992.tb01100.x>
70. Shen HY, De Schrijver S, Moonjai N, Verstrepen KJ, Delvaux F, Delvaux FR (2004) Effects of CO₂ on the formation of flavour volatiles during fermentation with immobilised brewer's yeast. *Appl Microbiol Biotechnol* 64:636–643. <https://doi.org/10.1007/s00253-003-1523-0>
71. Yang D (2019) Influence of top pressure on the flavor and sensorial characteristics of lager beer. *J Am Soc Brew Chem* 77:170–178. <https://doi.org/10.1080/03610470.2019.1603023>
72. Porras-Aguera JA, Roman-Camacho JJ, Moreno-Garcia J, Mauricio JC, Moreno J, Garcia-Martinez T (2020) Effect of endogenous CO₂ overpressure on the yeast “stressome” during the “prise de mousse” of sparkling wine. *Food Microbiol* 89:103431. <https://doi.org/10.1016/j.fm.2020.103431>

Publisher's Note Springer Nature remains neutral with regard to jurisdictional claims in published maps and institutional affiliations.